

Buffering Heavy Metal Ions with Photoactive CrownCast Cages

Hannah W. Mbatia,^[a] Daniel P. Kennedy,^[a] Casey E. Camire,^[a] Christopher D. Incarvito,^[b] and Shawn C. Burdette*^[a]

Keywords: Caged Compounds / Macrocycles / Fluorescent probes / Mercury / Lead

Historically, caged compounds have been used to interrogate the biological activity of organic molecules by using light; however, R. Tsien and others have developed methodologies over the last three decades for using nitrobenzyl-derived caged complexes to study the signaling behavior of Ca^{2+} . A series of cation-selective *N*-phenyl-azamacrocyclic receptors integrated with a 4,5-dimethoxy-2-nitrobenzyl (DMNB) photoactive group act as cages for divalent metal ions. The uncaging mechanism of these complexes involves a photoreaction that converts the nitrobenzhydrol, which is *para* to the aniline nitrogen atom, into the corresponding nitrosobenzophenone. Resonance delocalization of the aniline into the distal carbonyl group of the photoproduct attenuates the ability of the nitrogen atom to interact with the guest. CrownCast-1 (**3**) utilizes a 13-phenyl-1,4,7,10-tetraoxa-13-azacyclopentadecane (A15C5, **2**) receptor. Binding studies with CrownCast-1 revealed a modest selectivity for Ca^{2+} ; however, differences in the measured binding affinity upon photolysis suggest that CrownCast-1 is better suited to cage

Mg^{2+} . CrownCast-2 (**5**) is derived from the Hg^{2+} -selective 10-phenyl-1,4-dioxa-7,13-dithia-10-azacyclopentadecane (AT₂15C5, **4**) receptor. Aqueous binding studies demonstrate that CrownCast-2 binds tightly to Hg^{2+} , but the strong sulfur–mercury interactions in the complex mitigate the release of the metal ion upon photolysis. Based on previous reports of metal selectivity, CrownCast-3 (**7**), which possesses a 16-phenyl-1,4,7,10,13-pentaoxa-16-azacyclooctadecane (A18C6, **6**) receptor, was designed to act as a Pb^{2+} cage. Initial spectroscopic investigations suggest the uncaged ligand binds Pb^{2+} with higher affinity than the parent cage. To address this unexpected observation, a turn-on fluorescence sensor for Pb^{2+} that couples the A18C6 ligand with a 4,4-difluoro-4-bora-3a,4a-diaza-*s*-indacene (BODIPY) fluorophore was synthesized. In contrast to the titration data, photolysis of $[\text{Pb}(\text{CrownCast-3})]^{2+}$ in the presence of PbSensor-1 (**16**) demonstrates that the uncaged ligand, CrownUnc-3 (**15**), binds Pb^{2+} with a lower affinity than the caged *o*-nitrobenzhydrol macrocycle.

Introduction

The first use of nitrobenzyl protecting groups to mask the functions of phosphates was reported over 30 years ago.^[1,2] Subsequently, nitrobenzyl functionalities have become a powerful technique to interrogate the functions of amino acids,^[3] proteins,^[4] nucleotides,^[5,6] and steroids in biological systems.^[7] These tools are commonly referred to as cages because of their ability to prevent bioactive molecules from engaging in normal functions until they are released by using light.^[8–10] Since very few biological events in animals are driven by light, nitrobenzyl cages provide a convenient methodology to control the introduction of species into model systems with minimal interference.

In an analogous manner, two different strategies have been developed for releasing metal ions photochemically by using nitrobenzyl-based chelators. The first strategy uses photoinduced uncaging to initiate a carbon–heteroatom bond-cleavage reaction that fragments a multidentate ligand.^[11] The uncaging event increases free metal ion concentrations through the reduction of chelate effects. Alternatively, the uncaging reaction can introduce a carbonyl group *para* to a metal-bound aniline atom.^[12] After photolysis, the aniline nitrogen lone pair becomes resonance-delocalized onto the carbonyl group, which decreases the interaction between the metal ion and the nitrogen atom (Figure 1). By decreasing the bonding interaction, the binding affinity of the uncaged chelator is reduced. This strategy was initially developed by Tsien and co-workers to investigate Ca^{2+} signaling,^[13] and recently expanded to cage Zn^{2+} and other metal ions.^[14–16] All the caged complexes utilizing the attenuation of aniline ligand interactions consist of the receptor incorporated into a nitrobenzhydrol caging scaffold. We have coined the term *Cast* as a shorthand nomenclature for the nitrobenzhydrol class of cages since it is evocative of the casting out of the metal ion upon exposure to light.

[a] Department of Chemistry, University of Connecticut, 55 North Eagleville Road, Storrs, CT 06269-3060, USA
Fax: +1-860-486-2981
E-mail: shawn.burdette@uconn.edu

[b] Department of Chemistry, Yale University, 225 Prospect Street, P. O. Box 208107, New Haven, CT 06520-8107, USA

Supporting information for this article is available on the WWW under <http://dx.doi.org/10.1002/ejic.201000673>.

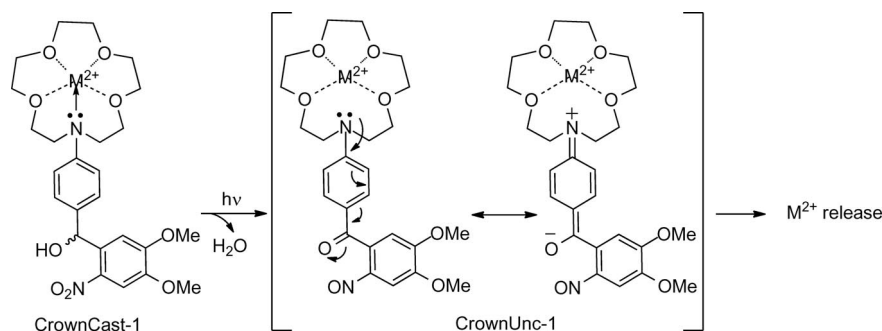


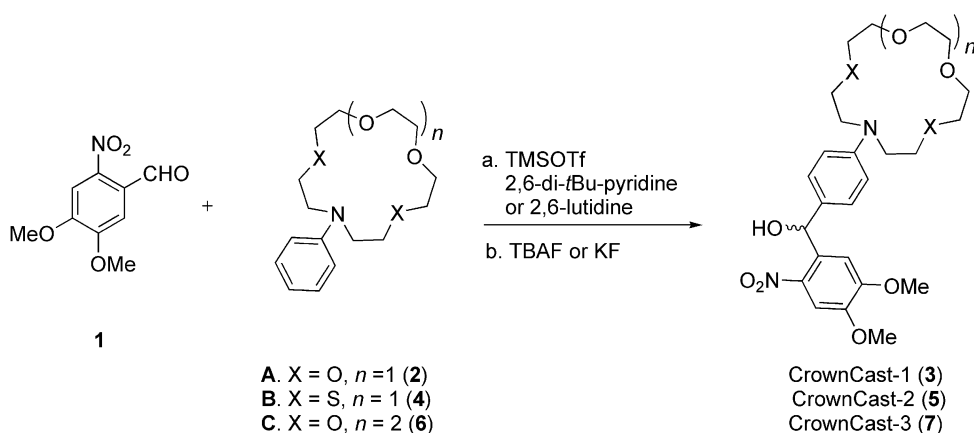
Figure 1. Uncaging action of Cast cages. Resonance delocalization of the anilino lone pair onto the carbonyl oxygen atom reduces the interaction between the nitrogen atom and the metal ion, which lowers the binding affinity.

Macrocyclic crown ethers are among the most recognizable receptors for metal ions; numerous sensors and molecular devices exploit the unique properties of these ligands.^[17–23] Initially, we designed a cage that utilized a 13-phenyl-1,4,7,10-tetraoxa-13-azacyclopentadecane receptor (A15C5, **2**) to develop new synthetic strategies for preparing Cast ligands.^[15] The crown ether macrocycle was chosen as a surrogate for other ligands that could potentially be incompatible with some of the synthetic manipulations being screened. During these studies, we discovered that the change in binding affinity between the caged and uncaged version of the CrownCast-1 (**3**) for certain divalent metal ions was almost an order of magnitude larger than that measured for glycol-bis(2-aminoethylether)-*N,N,N',N'*-tetraacetic acid (EGTA) based nitrobenzhydrol cages for Ca^{2+} . The name CrownCast incorporates the Cast nomenclature with a descriptor of the receptor. Although A15C5 does not preferentially interact with any particular metal ion, other macrocyclic ligands can more effectively discriminate between different guests based on the composition of the donor groups and the size of the cleft. Coupling of a more selective receptor with the uncaging behavior of the CrownCast system could therefore provide new caged complexes for biologically and environmentally important metal ions like Hg^{2+} and Pb^{2+} .

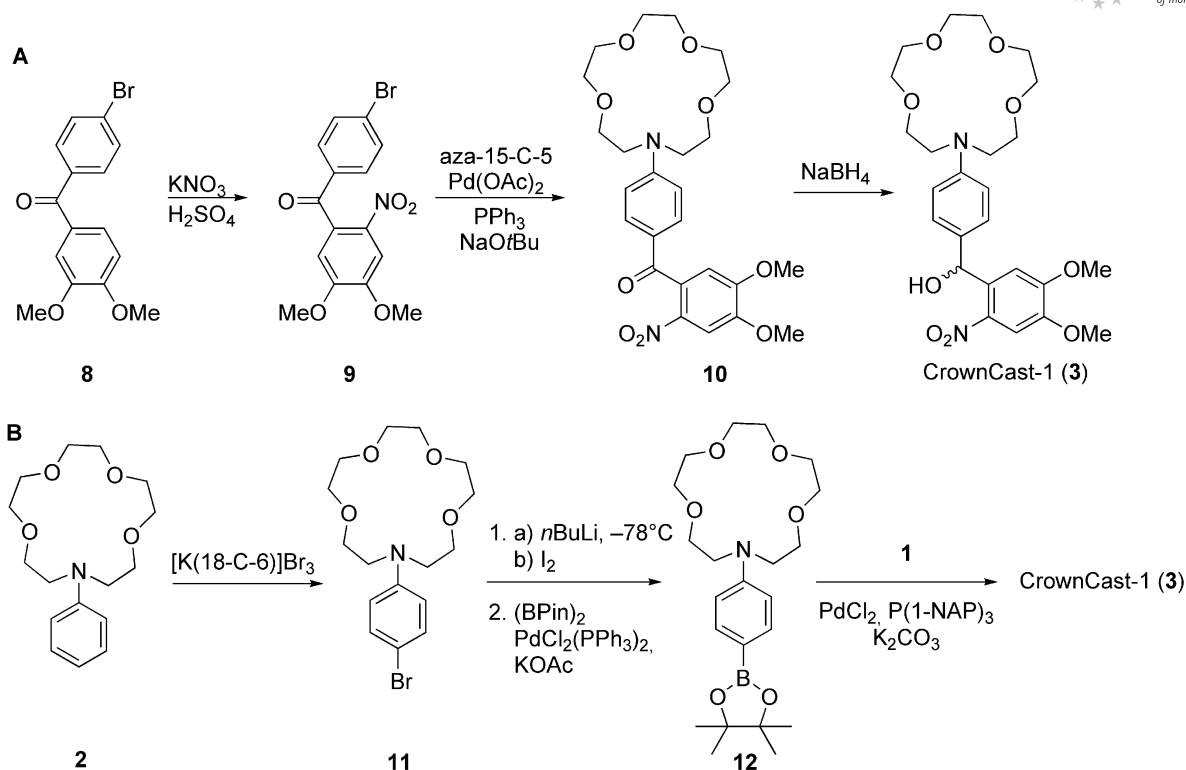
Results and Discussion

New Synthetic Methodologies Applied to the Synthesis of CrownCast-1

In a preliminary communication, we described three synthetic routes to CrownCast-1.^[15] The first utilizes the trimethylsilyl trifluoromethanesulfonate (TMSOTf) assisted electrophilic aromatic substitution reaction pioneered by Tsien and Zucker (Scheme 1, Entry A).^[12] According to the reported procedures, CrownCast-1 was prepared in 33% yield after the removal of the TMS group and purification. In our related work with ZinCast cages,^[14] we found that these methodologies were incompatible with some functional groups, so alternative synthetic procedures for accessing Cast cages were explored. The first alternative involves the assembly of a benzophenone scaffold, followed by reduction to the benzhydrol structure of CrownCast-1 (Scheme 2A). This strategy works well with ZinCast-1, but the yield of the reduction step in the presence of the A15C5 ligand is low, presumably because the reactivity of the BH_4^- anion is attenuated by binding of the sodium cation to the macrocycle. The final approach involves two successive Pd-catalyzed cross-coupling reactions^[24,25] to provide CrownCast-1 in 72% yield in four steps (Scheme 2B). The number



Scheme 1. Synthesis of CrownCast cages.



Scheme 2. New synthetic methodologies applied to the synthesis of CrownCast-1.

of steps in this route can be reduced to three by direct iodination of the aniline ring instead of bromination followed by a lithium/halogen exchange to introduce the iodine substituent. Whereas the one-step TMSOTf reaction remains the method of choice to prepare Cast cages, the Pd methodologies provide a practical alternative when this method cannot be used to access the desired structures.

Design and Synthesis of CrownCast-2 and CrownCast-3

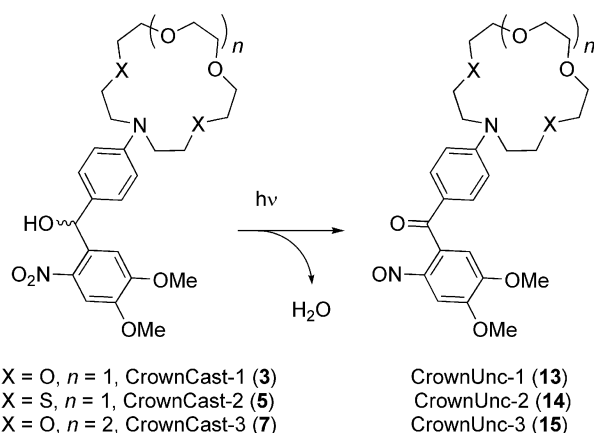
Replacement of the ether oxygen atoms in the 7- and 13-positions of A15C5 with thioethers provides the ligand 10-phenyl-1,4-dioxa-7,13-dithia-10-azacyclopentadecane (AT₂15C5, **4**). Several fluorescent sensors that are selective for Hg²⁺ have been constructed by using this receptor.^[20,21,26–38] The selectivity derives primarily from favorable sulfur–mercury interactions. In a manner analogous to our design rational of FerriCast for Fe³⁺,^[16] we reasoned that the established selectivity of the AT₂15C5 receptor in sensors would translate into a caged complex for Hg²⁺. In addition to heteroatom substitution, expansion of the A15C5 ring by one ethylene glycol unit provides the corresponding 16-phenyl-1,4,7,10,13-pentaoxa-16-azacyclooctadecane (A18C6, **6**) ligand. In the parent crown ethers, 15-crown-5 has a slight preference for Na⁺ over K⁺, whereas 18-crown-6 has the opposite selectivity.^[39,40] In the corresponding *N*-aryl-azamacrocycles, A18C6 has some preference for Pb²⁺,^[20] a large divalent metal ion, based on the size of the binding cavity. A CrownCast ligand containing

an A18C6 receptor could therefore act as a cage for Pb²⁺. Both Hg²⁺ and Pb²⁺ participate in deleterious interactions with biomolecules,^[41] and tools such as cages have the potential to provide insight into the mechanisms of these processes.

CrownCast-2 (**5**) and CrownCast-3 (**7**) were prepared in good yields by using the TMSOTf route (Scheme 1, Entries B and C). The Pd cross-coupling methodologies were not screened for CrownCast-2 owing to the possibility of catalyst poisoning by the thioether groups. In addition, the benzophenone route also proved impractical for preparing CrownCast-2 since poly(phosphoric acid) causes decomposition of the thioethers. Although the alternative methods were incompatible with the AT₂15C5 ligand, performing a dilute version of the TMSOTf reaction (0.01 M instead of 0.2 M), by using 2,6-lutidine as the base, and delivering the TMSOTf in small portions during the course of the reaction, the CrownCast-2 TMS ether was obtained in higher yields than when applying the originally reported procedures. Yields of CrownCast-3 were also higher by using these customized procedures. The modifications appear to reduce the formation of malachite green like byproducts,^[42] which are responsible for reduced yields of the desired products. The intermediate TMS ether precursor was converted into the desired benzhydrol upon treatment with F[−]. KF can be used as the source of F[−] instead of tetrabutylammonium fluoride (TBAF) in the deprotection of CrownCast-3 since the A18C6 receptor can act as a phase-transfer catalyst.

Uncaging Mechanism of CrownCast Cages

The exposure of the CrownCast ligands to light initiates a Norrish type II photoreaction that converts the benzhydryl into the corresponding benzophenone (Scheme 3).^[43–45] The conversion of the cage into the uncaged form can be quantified by monitoring the changes in the λ_{max} value of the CrownCast and CrownUnc (the uncaged, benzophenone version of the Cast ligands) that appear at $\lambda = 270$ and 350 nm, respectively. The CrownUnc benzophenone molecules absorb with higher extinction coefficients owing to the more conjugated aromatic backbone. In CH_3CN solution, by using $\lambda = 350$ nm with a 150 W source, the quantum yields of CrownCast-2 and CrownCast-3 were determined to be 3.4 and 1.7%, respectively (Table 1). Each CrownUnc was prepared in bulk by photolysis of the corresponding CrownCast to obtain the precise extinction coefficients of both the caged and uncaged ligand, which allows accurate measurements of the quantum yields by using spectrophotometric techniques. The quantum yields obtained for the two new apo-CrownCast ligands are comparable to both CrownCast-1 and other related nitrobenzhydryl derived cages.^[15,46]



Scheme 3. Synthesis of CrownUnc ligands.

Table 1. Quantum yields of photolysis for CrownCast ligands and their corresponding metal complexes in CH_3CN (25 μM) by using a 150 W Xe source at $\lambda = 350$ nm.

Compound/complex	ϵ [$\text{cm}^{-1} \text{M}^{-1}$] ($\lambda = 350$ nm)	$\phi_{\text{photolysis}}$ [%]	Efficiency $\phi \times \epsilon$
CrownCast-1	5300	0.5 ± 0.2	27
CrownCast-2	5000	3.4 ± 0.2	169
CrownCast-3	7200	1.7 ± 0.1	121
$[\text{Ca}(\text{CrownCast-1})]^{2+[\text{a}]}$	5300	0.7 ± 0.2	37
$[\text{Zn}(\text{CrownCast-1})]^{2+[\text{b}]}$	5300	1.6 ± 0.6	85
$[\text{Hg}(\text{CrownCast-2})]^{2+[\text{c}]}$	5000	4.2 ± 0.2	208
$[\text{Hg}(\text{CrownCast-3})]^{2+[\text{c}]}$	5700	3.2 ± 0.7	187
$[\text{Pb}(\text{CrownCast-3})]^{2+[\text{d}]}$	7200	4.0 ± 0.1	291

[a] $[\text{Ca}(\text{ClO}_4)_2] = 125 \mu\text{M}$ (5.0 equiv.). [b] $[\text{Zn}(\text{ClO}_4)_2] = 1.25 \mu\text{M}$ (50 equiv.). [c] $[\text{Hg}(\text{ClO}_4)_2] = 25 \mu\text{M}$ (1.0 equiv.). [d] $[\text{Pb}(\text{ClO}_4)_2] = 25 \mu\text{M}$ (1.0 equiv.). The CrownCast was saturated, but binding to the corresponding CrownUnc was negligible.

In the presence of metal ions, the quantum yields of all the CrownCast ligands increase slightly (Table 1), a typical property of this class of ligands.^[15,46] The metal ions screened correspond to those of the desired applications; therefore, Hg^{2+} was selected for CrownCast-2 and Pb^{2+} for CrownCast-3. Photolysis was carried out by using concentrations of M^{2+} in which binding to the corresponding photoproducts would be negligible, therefore allowing for direct spectrophotometric measurements of CrownUnc concentrations over the course of the photolysis. The limitation in using low-intensity illumination is the slow photolysis with a half-life of several hours. Typically, caged complexes are employed in biological investigations by using flash photolysis techniques.^[47] The flash techniques expose samples to a high number of photons on very short time scales. Future studies will address the photochemical properties of these and other related compounds with flash techniques.

Metal-Binding Properties of CrownCast-1 and -3

The interaction between the CrownCast cages with various divalent cations was assessed spectrophotometrically in CH_3CN (Table 2). Monitoring of the disappearance of the aniline-derived absorption band at $\lambda \approx 270$ nm allows the metal ion affinity of the cages to be quantified (Figure 2). In an analogous manner, the metal ion binding induced erosion of the charge-transfer band at $\lambda \approx 350$ nm in the CrownUnc derivatives allows the binding strength to be addressed.

In addition to the previously studied alkali earth metal ions Zn^{2+} and Cd^{2+} ,^[15] the interaction between CrownCast-1 with Hg^{2+} and Pb^{2+} was also investigated. Whereas the affinity for the heavy metals for the cage is similar in magnitude to that of Ca^{2+} , the change upon uncaging is significantly smaller than with the harder cations. While best described as a cage for Mg^{2+} in CH_3CN owing to the $\Delta K_d > 200$, the measurements indicate that CrownCast-1 behaves as a cage for all the divalent metal ions tested except Pb^{2+} , in which $\Delta K_d < 1$. A ΔK_d value of < 1 suggests the CrownUnc-1 binds more tightly than the caged ligand; however, two mitigating factors should be considered when interpreting this data. First, the spectrophotometric assay relies on the interaction between the aniline nitrogen atom and the metal ion guest. Whereas uncaging decreases the electron density on the nitrogen atom that weakens the donor ability, the unchanged crown ether ligand can still coordinate the metal ion. A softer Pb^{2+} ion in the receptor after uncaging may interact with the aniline nitrogen atom more readily than harder alkali earth metal ions. Second, the absorption of the CrownCast at $\lambda = 270$ nm appears to be a complicated feature, or combination of transitions, whereas the $\lambda \approx 350$ nm peak of the CrownUnc appears to be a well-behaved charge-transfer band associated with the benzophenone. These two factors may lead to deviation from expected spectroscopic behavior when the binding strength does not change significantly upon uncaging.

The metal-binding properties of CrownCast-3 with the heavier metal ions are similar to those observed in Crown-

Table 2. Dissociation constants [μM] of CrownCast cages and CrownUnc photoproducts with metal perchlorates in CH_3CN .^[a]

M^{n+}	$r_{\text{ion}} [\text{\AA}]^{[b]}$	CrownCast-1			CrownCast-2			CrownCast-3		
		Caged	Uncaged	ΔK_d	Caged	Uncaged	ΔK_d	Caged	Uncaged	ΔK_d
Na^+	1.02	1330 ± 10	NB ^[c]	NA ^[d]	NB	NB	NA	168 ± 4	NB	NA
K^+	1.38	3500 ± 100	NB	NA	NB	NB	NA	178 ± 1	NB	NA
Mg^{2+}	0.72	64 ± 7	13100 ± 700	205	NB	NB	NA	2050 ± 80	1550 ± 50	1.3
Ca^{2+}	1.00	14 ± 2	600 ± 100	43	NB	NB	NA	11.6 ± 0.1	8.8 ± 0.3	0.76
Sr^{2+}	1.18	48 ± 1	2200 ± 200	46	NB	NB	NA	9.78 ± 0.07	6.68 ± 0.06	0.68
Ba^{2+}	1.35	79 ± 3	3100 ± 100	39	NB	NB	NA	12.4 ± 0.6	7.80 ± 5	0.63
Zn^{2+}	0.74	161 ± 8	NB	NA	1200 ± 200	NB	NA	198 ± 5	NB	NA
Cd^{2+}	0.95	68 ± 1	NB	NA	520 ± 50	NB	NA	57.7 ± 0.9	165 ± 2	2.9
Hg^{2+}	1.19	8.1 ± 0.1	23 ± 3	2.8	6.9 ± 0.3	10.4 ± 0.5	1.5	6.8 ± 0.3	15.3 ± 0.1	2.3
Pb^{2+}	1.19	10.8 ± 0.3	8.4 ± 0.1	0.78	25 ± 5	1630 ± 30	65	11.3 ± 0.3	7.4 ± 0.1	0.65

[a] The 1:1 M/L binding constants were calculated with XLfit. [b] Ionic radii are for coordination number = 6. [c] No binding observed (NB): Metal binding was not observed when the ligand was exposed to >5000 equiv. of M^{2+} . [d] Not applicable (NA): The value for ΔK_d could not be accurately assessed, because no value for the K_d required to do the calculation was available.

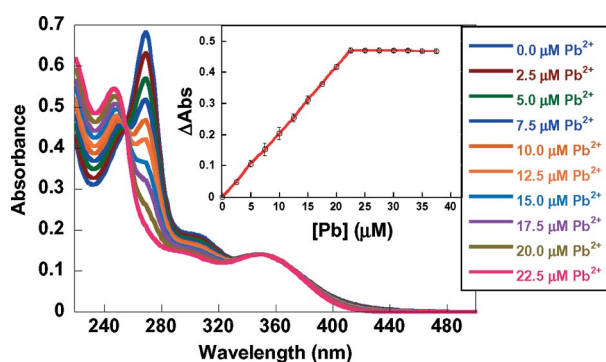
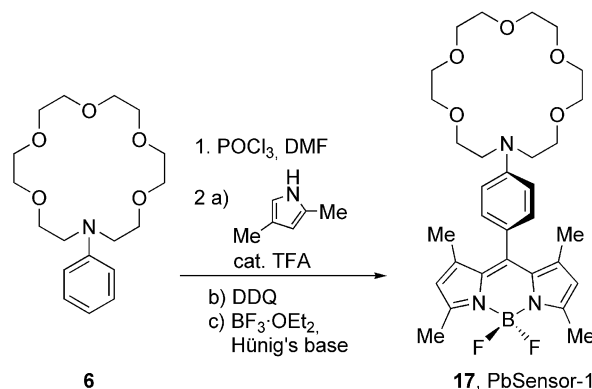


Figure 2. Titration of $25 \mu\text{M}$ CrownCast-3 with $\text{Pb}(\text{ClO}_4)_2$ in CH_3CN . The excess absorbance at $\lambda = 270 \text{ nm}$ was fitted to a 1:1 binding isotherm (inset). The error bars represent the variance in the measurements over three trials.

Cast-1, including the $\Delta K_d < 1$ for Pb^{2+} . Unexpectedly, however, the alkali earth metal ions also exhibited $\Delta K_d < 1$. To further probe the metal-ion binding properties of CrownCast-3, the A18C6 receptor was integrated with a BODIPY fluorophore to generate a novel turn-on fluorescent sensor for Pb^{2+} (17, PbSensor-1). Similar fluorescent sensors based on macrocyclic ligands have been reported,^[45] and we have shown that uncaging a metal ion using a fluorescent probe as a competitive ligand provides an independent demonstration of analyte release.^[14,16,48]

PbSensor-1 (17) was prepared by converting compound 6 into the corresponding aldehyde followed by assembly of the BODIPY sensor with the standard multi-step, one-pot procedure (Scheme 4).^[49] Metal ion binding to the A18C6 receptor of PbSensor-1 interrupts a charge transfer between the aniline moiety and the BODIPY fluorophore. PbSensor-1 exhibits a 1600-fold enhancement in the integrated fluorescence intensity when titrated with Pb^{2+} in CH_3CN . PbSensor-1 ($\lambda_{\text{max}} = 496 \text{ nm}$, $\epsilon = 88000 \text{ cm}^{-1} \text{ M}^{-1}$) is essentially nonfluorescent ($\phi \approx 0$), whereas $[\text{Pb}(\text{PbSensor-1})]^{2+}$ ($\lambda_{\text{max}} = 499 \text{ nm}$, $\epsilon = 89,000 \text{ cm}^{-1} \text{ M}^{-1}$) has an emission quantum yield of 0.74. Although heavy metal ions usually quench fluorescence, the decoupling of the aniline donor and the BODIPY fluorophore provided unique turn-on

sensors.^[19,50,51] The selectivity of PbSensor-1 was tested by recording the fluorescence output of the sensor in the presence of various cations (Figure 3). Of all the species screened only Sr^{2+} , Ba^{2+} , and Hg^{2+} illicit a response from the sensor. These competing species also interact strongly with CrownCast-3. An additional increase in emission is observed when excess Pb^{2+} is introduced into the solution containing competing metal ions. With the exception of the slight preference for Pb^{2+} , PbSensor-1 behaves identically to the analogous BODIPY sensors that utilize the A15C5 macrocycle instead of A18C6.^[50,51]



Scheme 4. Synthesis of PbSensor-1.

Photolysis of $12 \mu\text{M}$ $[\text{Pb}(\text{CrownCast-3})]^{2+}$ in the presence of $1.0 \mu\text{M}$ PbSensor-1 at $\lambda = 350 \text{ nm}$ with a 150 W source resulted in an increase in the measured fluorescence output (Figure 4). Emission enhancements observed during the photolysis indicated the in situ formation of the $[\text{Pb}(\text{PbSensor-1})]^{2+}$ complex, which has a K_d value of $0.93 \pm 0.01 \mu\text{M}$. Absorbance measurements during the photolysis indicate the formation of the apo-photoproduct CrownUnc-3 at $\lambda = 350 \text{ nm}$. This fluorescence assay indicates that the introduction of the carbonyl group in CrownUnc-3 does weaken the A18C6 receptor's affinity for Pb^{2+} compared to CrownCast-3, although the decrease cannot be quantified accurately by absorption spectroscopy.

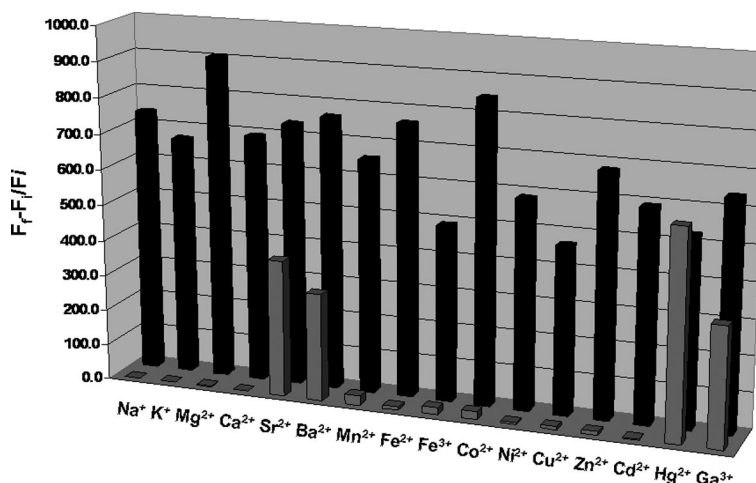


Figure 3. Fluorescence selectivity of PbSensor-1 (17) with 1.0 equiv. of M (gray bars) and 1.0 equiv. M^{n+} + 10 equiv. Pb^{2+} (black bars). The assay was carried out with 1.0 μM PbSensor in CH_3CN , λ_{ex} = 470 nm, λ_{em} = 480–650 nm.

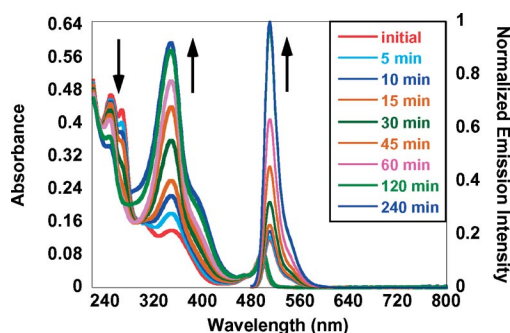


Figure 4. Photolysis of 25 μM CrownCast-3, 12 μM $Pb(ClO_4)_2$, and 1.0 μM PbSensor-1 (16) in CH_3CN with a 150 W source. The solution was photolyzed at $\lambda_{photolysis}$ = 350 nm, and the sensor excited at λ_{ex} = 470 nm (slit widths = 5.0 nm). The solution was equilibrated at 23 °C for 0.5 h prior to photolysis. The absorbance spectra are represented as thick lines with absorption features centered at $\lambda \approx 270$ and 350 nm and the emission spectra as thin lines with a $\lambda_{max} \approx 500$ nm.

Hg²⁺ Binding Properties of CrownCast-2

In CrownCast-2, the oxygen atoms closest to the aniline group are substituted for softer sulfur donors. As a result, minimal spectrophotometric changes in the spectrum of CrownCast-2 were observed upon saturation of the AT₂15C5 receptor with >5000 equiv. of various alkaline earth metal ions. The thioether ligands clearly provide the AT₂15C5 receptor with a strong preference for heavy metal ions over alkali and alkaline earth metal ions, although Pb^{2+} exhibits a $\Delta K_d < 1$ like CrownCast-1 and CrownCast-3. Unexpectedly, the ΔK_d of CrownCast-2 upon uncaging of Hg^{2+} is quite small (≈ 2). To further elucidate the origins of the modest ΔK_d values, we analyzed the Hg^{2+} complex of AT₂15C5 by X-ray crystallography. The $[Hg(AT_215C5)](ClO_4)_2$ structure serves as a model for the $[Hg(CrownCast-2)]^{2+}$ complex formed during the binding studies. The complex reveals that both Hg–S distances are

ca. 2.4 Å, whereas the Hg–N distances are ca. 0.15 Å longer, which is consistent with the thiophilic nature of Hg^{2+} . A stable dithioether– Hg^{2+} adduct, which is held in proximity to weaker ligands by the macrocyclic ligand, provides the most likely explanation for the modest ΔK_d value. We hypothesize that the thioether ligands force the interaction between the aniline nitrogen atom and the Hg^{2+} ion in CrownCast-2; therefore, uncaging does not significantly change the stability of the CrownUnc-2 complex.

Whereas neither CrownCast-1 nor CrownCast-3 bind any of the metal ions screened in aqueous solution, the AT₂15C5 receptor of CrownCast-2 binds Hg^{2+} in water. Although the binding is weaker and an organic cosolvent is required to maintain solubility of the ligand, CrownCast-2 behaves as an Hg^{2+} cage in aqueous solution (20 mM HEPES, 20% EtOH, pH = 7). The K_d value of the caged ligand is $15.3 \pm 0.5 \mu M$, and that of the uncaged ligand is $430 \pm 2 \mu M$, which gives a ΔK_d value of 28. None of the other divalent metal ions screened interfere with Hg^{2+} binding and the quantum yields remains constant {CrownCast-2: ϕ = 2.9%; $[Hg(CrownCast-2)]^{2+}$: ϕ = 3.3%}.

Titration were performed in buffered solutions at pH = 7;^[32,35] however, mM concentrations of K^+ and Na^+ interfere with the accurate measuring of the Hg^{2+} -induced changes in the absorption spectrum. Since both K^+ and Na^+ are abundant in biological systems, the practical applications of CrownCast-2 may be limited. Whereas others have demonstrated Hg^{2+} binding to AT₂15C5 in buffered solution, none of the experiments were carried out under simulated physiological conditions of constant ionic strength. Independent measurement of Na^+ and K^+ binding revealed that both interact very weakly with the macrocyclic ligand. Protonation of the aniline nitrogen atom could also interfere with metal ion binding in aqueous solution; however, the anilino nitrogen atom in related macrocyclic Cast cages has a $pK_a < 4$, which is consistent with measurements in similar systems.^[52–55]

Conclusion

Three members of the CrownCast family of metal ion cages and the respective photoproducts have been synthesized and characterized. Metal ion binding affinity and selectivity of the caged ligands is analogous to trends observed in unrelated chelators utilizing the same receptors. The basis of the selectivity and affinity depends on the match between the diameter of the metal cation and the size of the macrocyclic cavity. In addition, expected trends in hard–soft acid–base behavior are observed. Whereas the decrease in binding affinity upon uncaging reflects the decreased electron density on the aniline nitrogen atom, the nature of the other ligands greatly influences the magnitude of the change. In CrownCast-2 (Figure 5) for example, the two thioether ligands enhance the selectivity of the cage for Hg^{2+} , but also stabilize the metal complex sufficiently to force an interaction with the aniline nitrogen atom after uncaging. Thus, the ΔK_d value of CrownCast-2 with Hg^{2+} is low, which could limit its potential applications as a cage. The examination of X-ray structures with model ligands supports this hypothesis. Although none of the macrocycles prove ideal for aqueous applications, the analysis of the data gathered in this study will assist in the design of future caged complexes. The construction of cages suitable for investigating the detrimental biological activity of Hg^{2+} and Pb^{2+} is ongoing.

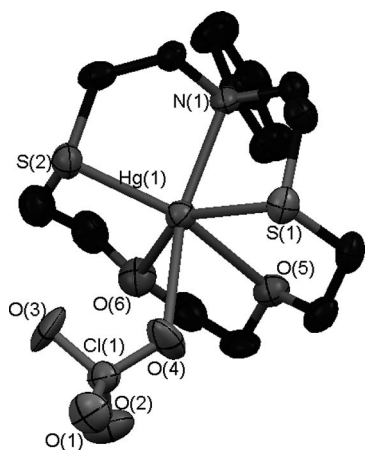


Figure 5. ORTEP diagram of the CrownCast-2 model complex $[\text{Hg}(\text{AT}_215\text{C}_5)(\text{ClO}_4)](\text{ClO}_4)$ showing 50% thermal ellipsoids. Hydrogen atoms and disordered, noncoordinating perchlorate anions are omitted for clarity.

Experimental Section

General Procedures: All the materials were of research grade or spectro-grade in the highest purity commercially available from Acros Organics or TCI America. Dichloromethane, toluene, and thf were sparged with argon and dried by passage through a Seca Solvent Purification System. All chromatography and TLC were performed on silica (230–400 mesh) from Silicycle unless otherwise specified. Activated basic alumina (ca. 150 mesh) was obtained from Acros Organics. TLC plates were developed with mixtures of EtOAc/hexanes or CH_2Cl_2 /methanol unless otherwise specified and

were visualized with $\lambda = 254$ and 365 nm light and I_2 or Br_2 vapor. ^1H and ^{13}C NMR spectra were recorded with a Bruker 400 MHz NMR instrument, and chemical shifts are reported in ppm on the δ scale relative to tetramethylsilane. IR spectra were recorded with a Nicolet 205 FT-IR instrument, and the samples were prepared as KBr pellets. High-resolution mass spectra were recorded at the University of Connecticut mass spectrometry facility with a micro-mass Q-Tof-2TM mass spectrometer operating in positive ion mode. The instrument was calibrated with Glu-fibrinopeptide B 10 pmol/ μL by using a 50:50 solution of $\text{CH}_3\text{CN}/\text{H}_2\text{O}$ with 0.1% acetic acid. The compounds 13-phenyl-1,4,7,10-tetraoxa-13-azacyclopentadecane (A15C5, **2**),^[56] 10-phenyl-1,4-dioxa-7,13-dithia-10-azacyclopentadecane (AT₂15C5, **4**),^[57] 16-phenyl-1,4,7,10,13-pentaoxa-16-azacyclooctadecane (A18C6, **6**),^[58] [4-(1,4,7,10-tetraoxa-13-azacyclopentadecane)phenyl]-(4,5-dimethoxy-2-nitrophenyl)-methanol (CrownCast-1, **3**),^[15] and [4-(1,4,7,10-tetraoxa-13-azacyclopentadecane)phenyl]-(4,5-dimethoxy-2-nitrosophenyl)-methanone (CrownUnc-1, **13**)^[15] were prepared as previously described.

(4,5-Dimethoxy-2-nitrophenyl)[4-(4,7-dioxa-1,10-dithia-13-azacyclooctadec-13-yl)phenyl]methanol (5, CrownCast-2): 2,6-Di-*tert*-butyl-4-methylpyridine (158 mg, 0.768 mmol) and TMSOTf (118 μL , 0.650 mmol) were added, in one portion, to a solution of **4** (164 mg, 0.500 mmol) and *ortho*-nitroveratraldehyde (**1**) (161 mg, 0.650 mmol) in CH_2Cl_2 (3.0 mL). The resulting dark blue/green solution was stirred at 23 °C for 16 h. The solution was diluted with CH_2Cl_2 (50 mL), washed with brine (50 mL), dried with MgSO_4 , filtered, and the solvents were evaporated to dryness. Flash chromatography on silica with EtOAc/petroleum ether (1:1) afforded 74 mg (24%) of the TMS ether as a yellow foam ($R_f = 0.31$). The TMS ether was dissolved in CH_2Cl_2 (3.0 mL), and TBAF (1 M) in THF (850 μL , 0.85 mmol) was added with stirring over 5 min. Flash chromatography on silica with EtOAc/petroleum ether (1:1) furnished **5** as yellow foam (60 mg, 92%). $R_f = 0.20$ (silica; EtOAc/petroleum ether, 1:1). ^1H NMR (400 MHz, CDCl_3): $\delta = 7.64$ (s, 1 H, phenyl H), 7.54 (s, 1 H, phenyl H), 7.19 (dd, $J = 8$ Hz, 2 H, phenyl H), 6.60 (dd, $J = 8$ Hz, 2 H, phenyl H), 6.50 (s, 1 H, OH), 4.01 (s, 3 H), 3.96 (s, 3 H), 3.83 (m, 4 H), 3.64 (m, 8 H), 2.88 (m, 4 H), 2.72 (m, 4 H), 2.49 (s, 1 H) ppm. ^{13}C NMR (100 MHz): $\delta = 153.6, 147.9, 146.8, 140.2, 135.0, 129.8, 128.7, 111.8, 110.3, 108.4, 74.5, 71.6, 71.0, 56.7, 56.6, 52.1, 31.4, 29.7$ ppm. IR (thin film): $\tilde{\nu} = 3474, 2915, 2886, 2858, 1606, 1512$ (ν_{as} NO_2), 1266 (ν_{s} NO_2) cm^{-1} . HRMS (ESI+): calcd. for MNa^+ 561.1705; found 561.1719.

(4,5-Dimethoxy-2-nitrophenyl)[4-(1,4,7,10,13-pentaoxa-16-azacyclooctadec-16-yl)phenyl]methanol (7, CrownCast-3): Compound **6** (554 mg, 1.00 mmol) in CH_2Cl_2 (100 mL) was added to a mixture of *ortho*-nitroveratraldehyde (**1**) (448 mg, 1.30 mmol) and 2,6-lutidine (284 μL , 1.50 mmol). TMSOTf (385 μL , 1.30 mmol) was added dropwise to the resulting solution at 23 °C. The reaction mixture was stirred for 1 h, before the addition of fresh aliquots of TMSOTf (385 μL , 1.30 mmol) and 2,6-lutidine (284 μL , 1.50 mmol). The mixture was stirred for a further 5 h. The reaction was quenched with water (100 mL), the organic phase isolated, and the aqueous phase extracted with CH_2Cl_2 (50 mL, $\times 3$). The organic fractions were pooled and concentrated to dryness. CH_3CN (5.0 mL) and KF (473 mg, 5.00 mmol) dissolved in a minimal amount of water (ca. 1 mL) were added to the residue. The reaction mixture was stirred for 12 h, concentrated to dryness, and the residue was dissolved in water (50 mL). The aqueous mixture was extracted with CH_2Cl_2 (50 mL, $\times 3$), the organic fractions were pooled, dried with an excess of MgSO_4 , and filtered by gravity. The filtrate was dried under vacuum and subjected to flash chromatography on basic alumina with neat EtOAc to furnish **7** as a yellow oil (538 mg, 60.1%). $R_f = 0.22$ (alumina; EtOAc). ^1H NMR

(400 MHz, CDCl₃): δ = 7.64 (s, 1 H, phenyl H), 7.54 (s, 1 H, phenyl H), 7.14 (dd, J = 8 Hz, 2 H, phenyl H), 6.62 (dd, J = 8 Hz, 2 H, phenyl H), 6.48 (s, 1 H, phenyl H), 4.19 (s, 3 H, OCH₃), 3.97 (s, 3 H, OCH₃), 3.67 (m, 24 H, OCH₂), 2.48 (s, 1 H, OH) ppm. ¹³C NMR (100 MHz): δ = 153.5, 147.9, 147.8, 140.0, 135.1, 129.5, 128.5, 111.6, 110.4, 108.3, 71.6, 71.0, 70.9, 68.9, 56.6, 56.6, 51.5 ppm. IR (thin film): $\tilde{\nu}$ = 3399, 2915–2860, 1610, 1513 (ν_{as} NO₂), 1267 (ν_{s} NO₂) cm⁻¹. HRMS (ESI+): calcd. for MNa⁺ 551.2605; found 551.2583.

(4,5-Dimethoxy-2-nitrosophenyl)[4-(4,7-dioxa-1,10-dithia-13-azacyclooctadec-13-yl)phenyl]methanone (14): A solution of **5** (21.6 mg, 40.1 μ mol) in CH₃CN (4.0 mL) sealed in a quartz cuvette was irradiated with a 1000 W source for 4 h. The solvent was removed under reduced pressure and subjected to flash chromatography on silica with EtOAc/hexanes (13:20) to furnish the product as an orange foam (20.4 mg, 97.6%). R_f = 0.28 (silica; EtOAc/hexanes, 13:20). ¹H NMR (400 MHz, CDCl₃): δ = 7.77 (dd, J = 8 Hz, 2 H, phenyl H), 7.14 (s, 1 H, phenyl H), 6.68 (dd, J = 10 Hz, 2 H, phenyl H), 6.34 (s, 1 H, phenyl H), 4.11 (s, 3 H, OCH₃), 4.05 (s, 3 H, OCH₃), 3.97 (m, 4 H, NCH₂), 3.82 (m, 8 H, OCH₂), 2.91 (m, 4 H, SCH₂), 2.89 (m, 4 H, SCH₂) ppm. ¹³C NMR (100 MHz): δ = 193.9, 160.1, 156.0, 151.4, 150.1, 140.2, 133.0, 127.2, 110.9, 109.9, 91.9, 74.6, 70.9, 57.0, 56.4, 52.2, 31.6, 29.6 ppm. IR (thin film): $\tilde{\nu}$ = 2921, 2854, 1645 (ν_{CO}), 1586 (ν_{NO}) cm⁻¹. HRMS (ESI+): calcd. for MNa⁺ 543.1600; found 543.1628.

(4,5-Dimethoxy-2-nitrosophenyl)[4-(1,4,7,10,13-pentaoxa-16-azacyclooctadec-16-yl)phenyl]methanone (15): Prepared from **7** according to the same procedure as that for **14**. Compound **15** was obtained as a yellow oil (48 %). R_f = 0.32 (alumina; EtOAc). ¹H NMR (400 MHz, CDCl₃): δ = 7.74 (dd, J = 10 Hz, 2 H, phenyl H), 7.14 (s, 1 H, phenyl H), 6.63 (dd, J = 10 Hz, 2 H, phenyl H), 6.33 (s, 1 H, phenyl H), 4.28 (s, 3 H, OCH₃), 4.23 (s, 3 H, OCH₃), 3.70 (m, 24 H, OCH₂) ppm. ¹³C NMR (100 MHz): δ = 193.8, 160.1, 156.0, 152.4, 150.1, 140.4, 132.8, 126.9, 110.8, 109.9, 91.8, 71.1, 71.03, 70.99, 70.96, 68.6, 57.0, 56.4, 51.7 ppm. IR (thin film): $\tilde{\nu}$ = 2920–2864, 1645 (ν_{CO}), 1586 (ν_{NO}) cm⁻¹. HRMS (ESI+): calcd. for MNa⁺ 555.2319; found 555.2311.

4-(1,4,7,10,13-Pentaoxa-16-azacyclooctadec-16-yl)benzaldehyde (16): POCl₃ (0.60 mL, 6.5 mmol, 2.0 equiv.) was added dropwise to a chilled solution (4 °C) of 16-phenyl-1,4,7,10,13-pentaoxa-16-azacyclooctadecane (**6**) (1.11 g, 3.27 mmol) in DMF (10.0 mL). The solution was warmed to 23 °C and stirred for 16 h. The resulting pale blue-green solution was diluted with iced water (50 mL). The pH was adjusted to 6.4–6.8 by the addition of solid K₂CO₃ and the heterogeneous mixture extracted with EtOAc (2 \times 50 mL). The organic fractions were pooled, dried with excess MgSO₄, filtered, and the filtrate was concentrated to dryness under vacuum. Flash chromatography on silica with CH₂Cl₂/CH₃OH (19:1) furnished the product as a pale-yellow oil (1.04 g, 86.9%). R_f = 0.5 (silica; CH₂Cl₂/CH₃OH, 19:1). ¹H NMR (400 MHz, CDCl₃): δ = 9.73 (s, 1 H, CHO), 7.72 (dd, J = 12 Hz, 2 H, aromatic H), 6.74 (dd, J = 16 Hz, 2 H, aromatic H), 3.74 [s, 4 H, N(CH₂CH₂)₂], 3.67 (s, 20 H, CH₂) ppm. ¹³C NMR (100 MHz): δ = 190.3, 152.9, 132.3, 125.5, 111.2, 71.1, 71.0, 71.0, 70.9, 68.6, 51.7 ppm. IR (thin film): $\tilde{\nu}$ = 2867, 2735, 1677, 1546, 1525, 1171, 1119 cm⁻¹. HRMS (ESI+): calcd. for MNa⁺ 390.1893; found 390.1923.

4,4-Difluoro-1,3,5,7-tetramethyl-8-(16-phenyl-1,4,7,10,13-pentaoxa-16-azacyclooctadec-16-yl)-4-bora-3a,4a-diaza-s-indacene (17): A solution of **16** (1.01 g, 2.76 mmol) in CH₂Cl₂ (300 mL) was degassed with a gentle stream of N₂ for 15 min, and 2,4-dimethylpyrrole (625 μ L, 6.07 mmol, 2.20 equiv.) and TFA (30 μ L, 15 mol-%)

were added. The resulting red solution was stirred at 23 °C for 2 h. TLC analysis indicated formation of the corresponding dipyrromethane (R_f = 0.20; silica; 5% CH₃OH/CH₂Cl₂). Then 2,3-dichloro-5,6-dicyanoquinone (ddq; 688 mg, 3.03 mmol, 1.10 equiv.) was added causing the immediate formation of a dark purple solution. After 1 h, TLC analysis indicated formation of the dipyrin (R_f \approx 0). Hünig's base (6.0 mL, 34.4 mmol) was slowly added to the solution, and small amounts of a highly colored solid precipitated from the solution. BF₃·OEt₂ (6.0 mL, 47.3 mmol) was added dropwise to the mixture. After 3 h, the mixture was analyzed by TLC, and the desired BODIPY compound was observed as an orange-colored spot (R_f = 0.5). The solution was washed with brine (100 mL), the biphasic mixture filtered by vacuum, the organic phase isolated, dried with an excess of MgSO₄, filtered, and the filtrate concentrated to dryness. The residue was adsorbed onto a minimal amount of silica and firstly subjected to flash chromatography on silica (50 g) with a gradient of 0–5% CH₃OH/CH₂Cl₂, before chromatography on a plug of basic alumina with a gradient of 0–2% CH₃OH in CH₂Cl₂ provided a nearly pure compound. The isolated compound was recrystallized from boiling CH₃OH (30 mL) to furnish the desired compound as a bright orange crystalline solid (90 mg, 5.6%). M.p. > 260 °C (decomp.) ¹H NMR (400 MHz, CDCl₃): δ = 7.01 (dd, J = 8 Hz, 2 H, aromatic H), 6.75 (dd, J = 8 Hz, 2 H, aromatic H), 5.96 (s, 2 H, 2,6-H BODIPY), 3.74 [t, J = 8.0 Hz, 4 H, N(CH₂CH₂)₂], 3.67 (m, 20 H, CH₂), 2.54 (s, 6 H, methyl H), 1.49 (s, 6 H, methyl H) ppm. ¹³C NMR (100 MHz): δ = 154.8, 148.5, 143.3, 132.3, 129.1, 122.0, 121.0, 112.0, 71.0, 70.9, 68.7, 51.4, 14.9, 14.7 ppm. IR (thin film): $\tilde{\nu}$ = 2958, 2903, 2869, 1609, 1543, 1524, 1513, 1190, 1157, 1081, 973 cm⁻¹. HRMS (ESI+): calcd. for MNa⁺ 608.3083; found 608.3061.

General Spectroscopic Methods: All solutions were prepared with spectrophotometric grade solvents. The metal perchlorate salts were obtained from Stem or EM Science and used as received. Absorption spectra were recorded with a Cary 50 UV/Vis spectrophotometer under the control of a Pentium IV based PC running the manufacturer-supplied software package. Spectra were routinely acquired at 25 °C, in 1-cm path length quartz cuvettes with a total volume of 3.0 mL. Analytical photolysis measurements were performed with a Hitachi F-4500 spectrophotometer under the control of a Pentium IV PC running the FL Solutions 2.0 software package. Excitation was provided by a 150 W Xe lamp (Ushio Inc.) operating at a current of 5 A. Photolysis reactions were conducted at 25 °C, in 1 cm quartz cuvettes with a total volume of 3.0 mL by using, unless otherwise stated, 10 nm slit widths and a photomultiplier tube power of 700 V. Preparative scale photolysis measurements were carried out by using a 1000 W Xe small-arc lamp. Solutions of **3**, **5**, and **7** (ca. 20–40 mg) in CH₃CN (4.0 mL) were irradiated in a 1 cm quartz cuvette for 4 h and the conversion checked periodically by TLC. Quantum yields of fluorescence^[59] and photolysis^[15,16] were measured according to reported procedures.

Binding Constants: Stock solutions of CrownCast-1, -2, or -3, CrownUnc-1, -2, or -3 and the metal perchlorate salts of Na⁺, K⁺, Mg²⁺, Ca²⁺, Sr²⁺, Ba²⁺, Zn²⁺, Cd²⁺, Hg²⁺, and Pb²⁺ were prepared in mM concentration in spectrophotometric grade CH₃CN. A 25 μ M solution of the ligand was prepared in 3000 μ L of CH₃CN and titrated in triplicate with each of the metal salt stock solutions. Absorbance spectra were corrected for dilution by multiplying the measured absorbance by Equation (1):

$$(V_0 - V_{\text{add}})/V_0 \quad (1)$$

in which V_0 is the initial volume and V_{add} is the added volume of the titrant. The conditional dissociation constant (K_d) was calcu-

lated by fitting data with the linear least-squares fitting program XLfit.^[60]

Collection and Reduction of X-ray Data: Structural analysis was carried out at the X-ray Crystallographic Facility at Yale University. Crystals were covered with oil, and a colorless plate with approximate dimensions of $0.10 \times 0.10 \times 0.10$ mm was mounted on a glass fiber at room temperature and transferred to a Rigaku RAXIS RAPID imaging plate area detector with graphite-monochromated Cu- K_{α} radiation ($\lambda = 1.54187$ Å) controlled by a PC running the Rigaku CrystalClear software package.^[61] The data were collected at a temperature of -180 ± 1 °C to a maximum 2θ value of 136.5° . The data were corrected for Lorentz and polarization effects. The structure was solved by direct methods^[62] and expanded by using Fourier techniques.^[63] The space group was determined by examining systematic absences and confirmed by the successful solution and refinement of the structure. The non-hydrogen atoms were refined anisotropically. Hydrogen atoms were refined by using the riding model. All calculations were performed by using the CrystalStructure crystallographic software package except for refinement,^[64] which was performed by using SHELXL-97.^[62] Selected crystallographic information is summarized in Tables 3 and 4, and a 50% thermal ellipsoid plot is shown in Figure 5. CCDC-784279 contains the supplementary crystallographic data for this paper. These data can be obtained free of charge from The Cambridge Crystallographic Data Centre via www.ccdc.cam.ac.uk/data_request/cif.

Table 3. Crystallographic parameters for $[\text{Hg}(\text{AT}_2\text{I}5\text{C}5)(\text{ClO}_4)]-(\text{ClO}_4)$.

Empirical formula	$\text{C}_{18}\text{H}_{28}\text{Cl}_2\text{HgN}_2\text{O}_{10}\text{S}_2$
Formula mass	768.04
Space group	$P2_1/c$
a [Å]	17.015(2)
b [Å]	9.8744(13)
c [Å]	14.9947(19)
α [°]	90
β [°]	92.022(3)
γ [°]	90
V [Å ³]	2517.7(6)
Z	4
$\rho_{\text{calcd.}}$ [g cm ⁻³]	2.026
μ [cm ⁻¹]	65.627
T [K]	223
Total no. data	15846
No. unique data	5679
Observed data ^[a]	5679
No. parameters	348
R [%] ^[b]	0.0750
$wR2$ [%] ^[c]	0.1173
Max/min peaks [e/Å]	1.32/−1.10

[a] Observation criterion: $I > 2\sigma(I)$. [b] $R = \Sigma ||F_o| - |F_c|| / \Sigma |F_o|$. [c] $wR2 = \{\Sigma [w(F_o^2 - F_c^2)^2] / \Sigma w(F_c^2)^2\}^{1/2}$.

Supporting Information (see footnote on the first page of this article): ¹H and ¹³C NMR spectroscopic data of all new compounds; absorption data, difference spectrum and fitting of binding isotherm for all titrations of CrownCast and CrownUnc ligands with all metal ions screened; absorption changes in CrownCast ligands and $[\text{M}(\text{CrownCast})]^{2+}$ upon irradiation with light used to calculate quantum yields; fluorescence titration and binding isotherm for Pb^{2+} and PbSensor-1.

Table 4. Selected interatomic distances [Å] and angles [°] for $[\text{Hg}(\text{AT}_2\text{I}5\text{C}5)(\text{ClO}_4)]-(\text{ClO}_4)$.

Hg(1)–S(1)	2.417(2) ^[a]	S(1)–Hg(1)–S(2)	139.15(9) ^[a]
Hg(1)–S(2)	2.413(2)	S(1)–Hg(1)–N(1)	83.66(18)
Hg(1)–N(1)	2.550(7)	S(1)–Hg(1)–O(4)	84.5(2)
Hg(1)–O(4)	2.612(12)	S(1)–Hg(1)–O(5)	76.42(16)
Hg(1)–O(5)	2.515(6)	S(1)–Hg(1)–O(6)	141.90(17)
Hg(1)–O(6)	2.464(6)	S(2)–Hg(1)–N(1)	83.23(18)
		S(2)–Hg(1)–O(4)	110.0(2)
		S(2)–Hg(1)–O(5)	143.16(16)
		S(2)–Hg(1)–O(6)	78.78(17)
		N(1)–Hg(1)–O(5)	94.7(2)
		N(1)–Hg(1)–O(6)	101.9(2)
		O(5)–Hg(1)–O(6)	65.6(2)

[a] Estimated standard deviations in the last digit(s). Atom labels are provided in Figure 5.

Acknowledgments

This work was supported by the University of Connecticut, the University of Connecticut Research Foundation (grant PD09-0154) and the by National Science Foundation (NSF) (grant CHE-0955361).

- [1] J. Engels, E.-J. Schlaeger, *J. Med. Chem.* **1977**, *20*, 907–911.
- [2] J. H. Kaplan, B. Forbush III, J. F. Hoffman, *Biochemistry* **1978**, *17*, 1929–1935.
- [3] E. M. Callaway, L. C. Katz, *Proc. Natl. Acad. Sci. USA* **1993**, *90*, 7661–7665.
- [4] M. Ghosh, I. Ichetovkin, X. Y. Song, J. S. Condeelis, D. S. Lawrence, *J. Am. Chem. Soc.* **2002**, *124*, 2440–2441.
- [5] S. Shah, S. Rangarajan, S. H. Friedman, *Angew. Chem. Int. Ed.* **2005**, *44*, 1328–1332.
- [6] X. J. Tang, I. J. Dmochowski, *Mol. Biosyst.* **2007**, *3*, 100–110.
- [7] S. Watanabe, M. Iwamura, *J. Org. Chem.* **1997**, *62*, 8616–8617.
- [8] L. Sjulson, G. Miesenbock, *Chem. Rev.* **2008**, *108*, 1588–1602.
- [9] H. M. Lee, D. R. Larson, D. S. Lawrence, *ACS Chem. Biol.* **2009**, *4*, 409–427.
- [10] H. T. Yu, J. B. Li, D. D. Wu, Z. J. Qiu, Y. Zhang, *Chem. Soc. Rev.* **2010**, *39*, 464–473.
- [11] G. C. R. Ellis-Davies, J. H. Kaplan, *J. Org. Chem.* **1988**, *53*, 1966–1969.
- [12] R. Y. Tsien, R. S. Zucker, *Biophys. J.* **1986**, *50*, 843–853.
- [13] S. R. Adams, J. P. Y. Kao, G. Gryniewicz, A. Minta, R. Y. Tsien, *J. Am. Chem. Soc.* **1988**, *110*, 3212–3220.
- [14] C. Gwizdala, D. P. Kennedy, S. C. Burdette, *Chem. Commun.* **2009**, 6967–6969.
- [15] D. P. Kennedy, C. Gwizdala, S. C. Burdette, *Org. Lett.* **2009**, *11*, 2587–2590.
- [16] D. P. Kennndy, C. D. Incarvilo, S. C. Burdette, *Inorg. Chem.* **2010**, *49*, 916–923.
- [17] J. S. Bradshaw, R. M. Izatt, *Acc. Chem. Res.* **1997**, *30*, 338–345.
- [18] A. J. Pearson, W. J. Xiao, *J. Org. Chem.* **2003**, *68*, 5361–5368.
- [19] K. Rurack, M. Kollmannsberger, U. Resch-Genger, J. Daub, *J. Am. Chem. Soc.* **2000**, *122*, 968–969.
- [20] D. Jimenez, R. Martinez-Manez, F. Sancenon, J. V. Ros-Lis, J. Soto, A. Benito, E. Garcia-Breijo, *Eur. J. Inorg. Chem.* **2005**, 2393–2403.
- [21] J. V. Ros-Lis, R. Martinez-Manez, F. Sancenon, J. Soto, M. Spieles, K. Rurack, *Chem. Eur. J.* **2008**, *14*, 10101–10114.
- [22] M. Verma, A. F. Chaudhry, M. T. Morgan, C. J. Fahrni, *Org. Biomol. Chem.* **2010**, *8*, 363–370.
- [23] S. Yoon, A. E. Albers, A. P. Wong, C. J. Chang, *J. Am. Chem. Soc.* **2005**, *127*, 16030–16031.
- [24] T. Yamamoto, T. Ohta, Y. Ito, *Org. Lett.* **2005**, *7*, 4153–4155.
- [25] T. Ishiyama, M. Murata, N. Miyaura, *J. Org. Chem.* **1995**, *60*, 7508–7510.

- [26] A. B. Descalzo, R. Martinez-Manez, R. Radeaglia, K. Rurack, J. Soto, *J. Am. Chem. Soc.* **2003**, *125*, 3418–3419.
- [27] M. C. Aragoni, M. Arca, A. Bencini, A. J. Blake, C. Caltagirone, A. Decortes, F. Demartin, F. A. Devillanova, E. Faggi, L. S. Dolci, A. Garau, F. Isaia, V. Lippolis, L. Prodi, C. Wilson, B. Valtancoli, N. Zaccheroni, *Dalton Trans.* **2005**, 2994–3004.
- [28] J. V. Ros-Lis, R. Martinez-Manez, J. Soto, *Org. Lett.* **2005**, *7*, 2337–2339.
- [29] A. Coskun, E. U. Akkaya, *J. Am. Chem. Soc.* **2006**, *128*, 14474–14475.
- [30] M. W. Glenny, L. G. A. van de Water, J. M. Vere, A. J. Blake, C. Wilson, W. L. Driessen, J. Reedijk, M. Schroder, *Polyhedron* **2006**, *25*, 599–612.
- [31] B. Garcia-Acosta, R. Martinez-Manez, F. Sancenon, J. Soto, K. Rurack, M. Spieles, E. Garcia-Breijo, L. Gil, *Inorg. Chem.* **2007**, *46*, 3123–3135.
- [32] M. J. Yuan, Y. L. Li, J. B. Li, C. H. Li, X. F. Liu, J. Lv, J. L. Xu, H. B. Liu, S. Wang, D. Zhu, *Org. Lett.* **2007**, *9*, 2313–2316.
- [33] E. V. Tulyakova, O. A. Fedorova, Y. V. Fedorov, G. Jonusauskas, L. G. Kuz'mina, J. A. K. Howard, A. V. Anisimov, *Russ. Chem. Bull.* **2007**, *56*, 513–526.
- [34] M. Zhu, M. J. Yuan, X. F. Liu, J. L. Xu, J. Lv, C. S. Huang, H. B. Liu, Y. L. Li, S. Wang, D. B. Zhu, *Org. Lett.* **2008**, *10*, 1481–1484.
- [35] M. Q. Tian, H. Ihmels, *Chem. Commun.* **2009**, 3175–3177.
- [36] S. Atilgan, I. Kutuk, T. Ozdemir, *Tetrahedron Lett.* **2010**, *51*, 892–894.
- [37] T. Abalos, D. Jimenez, M. Moragues, S. Royo, R. Martinez-Manez, F. Sancenon, J. Soto, A. M. Costero, M. Parra, S. Gil, *Dalton Trans.* **2010**, *39*, 3449–3459.
- [38] R. Guliyev, A. Coskun, E. U. Akkaya, *J. Am. Chem. Soc.* **2009**, *131*, 9007–9013.
- [39] K. V. Heyen, E. Cielén, A. Tahri, A. Saleh, N. Boens, G. J. Hoornaert, *Tetrahedron* **1999**, *55*, 5207–5226.
- [40] A. Tahri, E. Cielén, K. J. Van Aken, G. J. Hoornaert, F. C. De Schryver, N. Boens, *J. Chem. Soc. Perkin Trans. 2* **1999**, 1739–1748.
- [41] A. M. Florea, D. Busselberg, *Biomaterials* **2006**, *19*, 419–427.
- [42] F. Schweizer, B. Muehlethaler, *Farbe Lack* **1968**, *74*, 1159–1173.
- [43] C. G. Bochet, *J. Chem. Soc. Perkin Trans. 1* **2002**, 125–142.
- [44] J. E. T. Corrie, A. Barth, V. R. N. Munasinghe, D. R. Trentham, M. C. Hutter, *J. Am. Chem. Soc.* **2003**, *125*, 8546–8554.
- [45] M. Gaplovsky, Y. V. Il'ichev, Y. Kamdzhilov, S. V. Kombarova, M. Mac, M. A. Schworer, J. Wirz, *Photochem. Photobiol. Sci.* **2005**, *4*, 33–42.
- [46] S. R. Adams, J. P. Y. Kao, G. Gryniewicz, A. Minta, R. Y. Tsien, *J. Am. Chem. Soc.* **1988**, *110*, 3212–3220.
- [47] A. M. Gurney, H. A. Lester, *Physiol. Rev.* **1987**, *67*, 583–617.
- [48] D. H. M. Bandara, D. P. Kennedy, E. Akin, C. D. Incarvito, S. C. Burdette, *Inorg. Chem.* **2009**, *48*, 8445–8455.
- [49] G. Ulrich, R. Ziessel, A. Harriman, *Angew. Chem. Int. Ed.* **2008**, *47*, 1184–1201.
- [50] M. Kollmannsberger, K. Rurack, U. Resch-Genger, J. Daub, *J. Phys. Chem. A* **1998**, *102*, 10211–10220.
- [51] M. Kollmannsberger, K. Rurack, U. Resch-Genger, W. Rettig, J. Daub, *Chem. Phys. Lett.* **2000**, *329*, 363–369.
- [52] A. B. Descalzo, H.-J. Xu, Z.-L. Xue, K. Hoffmann, Z. Shen, M. G. Weller, X.-Z. You, K. Rurack, *Org. Lett.* **2008**, *10*, 1581–1584.
- [53] M. Maus, K. Rurack, *New J. Chem.* **2000**, *24*, 677–686.
- [54] K. Rurack, M. Kollmannsberger, J. Daub, *New J. Chem.* **2001**, *25*, 289–292.
- [55] Z. Shen, H. Roehr, K. Rurack, H. Uno, M. Spieles, B. Schulz, G. Reck, N. Ono, *Chem. Eur. J.* **2004**, *10*, 4853–4871.
- [56] Z. Zhou, F. Li, T. Yi, C. Huang, *Tetrahedron Lett.* **2007**, *48*, 6633–6636.
- [57] T. Abalos, D. Jimenez, R. Martinez-Manez, J. V. Ros-Lis, S. Royo, F. Sancenon, J. Soto, A. M. Costero, S. Gil, M. Parra, *Tetrahedron Lett.* **2009**, *50*, 3885–3888.
- [58] J. P. Dix, F. Voegtli, *Chem. Ber.* **1980**, *113*, 457–470.
- [59] A. T. R. Williams, S. A. Winfield, J. N. Miller, *Analyst* **1983**, *108*, 1067–1071.
- [60] *XLfit*, 5.1.0.0, ID Business Solutions Limited, Guildford, United Kingdom, **2009**.
- [61] *CrystalClear and CrystalStructure*, Rigaku/MSO, The Woodlands, TX, **2005**.
- [62] G. M. Sheldrick, *SHELX97*, **1997**.
- [63] P. T. Beurskens, G. Admiraal, G. Beurskens, W. P. Bosman, R. de Gelder, R. Israel, J. M. M. Smits, *DIREDF99*, University of Nijmegen, The Netherlands, **1999**.
- [64] *CrystalStructure 3.8: Crystal Structure Analysis Package*, Rigaku and Rigaku Americas, The Woodlands, TX, **2007**.

Received: June 22, 2010

Published Online: September 29, 2010